Proceedings of the 8th International Conference on Frontiers of Design and Manufacturing
Sept. 23~26, 2008, Tianjin, China

Modal Parameter Identification from Output-only Measurement Data: Application to Operating Spindle Condition Monitoring

Ruqiang Yan and Robert X. Gao
Department of Mechanical and Industrial Engineering, University of Massachusetts, Amherst, MA 01003, USA
e-mail: ryan@ecs.umass.edu; gao@ecs.umass.edu

Li Zhang
Global Research Center, General Electric Corporation, Niskayuna, NY 12309, USA
e-mail: zhangli@ge.com

Kang B. Lee
Manufacturing Metrology Division, National Institute of Standards and Technology, Gaithersburg, MD 20899, USA
e-mail: kang.lee@nist.gov

Abstract: This paper presents an experimental investigation of the dynamics of a custom-designed spindle test system under different operation conditions and at various stages of its service life. Unlike *classical modal analysis* techniques where known input excitation from hammer strikes are employed to excite the spindle, the presented *output-only modal analysis* method applies the stochastic subspace identification algorithm to the spindle response measured during its operation such that the modal parameters of the spindle as well as their variation are identified. This method accounts for the structural excitations during the spindle's operation, which are not considered if the spindle remains stationary in the experiment. The obtained modal parameters provide insight into structural changes of the spindle during its service life, and can be used as indicators for enhanced spindle condition monitoring.

Keywords: Spindle Dynamics, Output-only Modal Analysis, Stochastic Subspace Identification, Condition Monitoring

1 Introduction

Spindles are essential components of most machine tools. Identifying and monitoring vibrating characteristics (i.e., mode parameters) of spindle structure are necessary for health diagnosis in the future generation of "smart" machine tools. Modal parameter identification on non-rotating spindles has been performed by various researchers using hammer strikes to generate defined inputs [1-3]. Through mathematical modeling, researchers have found that the modal parameters of a spindle change in accordance with its operating conditions. As examples, the natural frequency of a spindle was seen to fluctuate periodically with the shaft speeds and its harmonics [4], and stiffer spring characteristics due to a high axial preload on the bearing have resulted in higher natural frequencies [5,6]. Identifying such parameter changes during a spindle's operation can as well provide insight into the spindle's present working status and its future performance, as the spindle degrades due to wear and tear. Such insight can also help devise more effective and efficient signal processing algorithms, e.g., by selecting proper scales needed for signal decomposition using the wavelet transform [7].

However, based on experimental observations from a realistic, custom-built spindle test system, the rotating spindle's response to instrumented hammer strikes was often overwhelmed by noise contamination. Figure 1a illustrates such an example of the measured output vibration signal from the spindle. Its corresponding correlation with the input hammer strike is weak, as indicated by an average value of less than 0.5 in the coherence function between each frequency component of the input and output signals (Figure 1b). Such low coherence values imply that a valid Frequency Response Function (FRF) of the spindle system cannot be derived, thus affecting the accuracy of the identified mode parameters if the classical modal analysis technique is applied. Furthermore, striking a rotating spindle is invasive and generally not acceptable due to interference with production and potential damage to the machine tool. This motivates the investigation of new techniques that could better enable modal parameter identification of a rotating spindle under changing operation conditions and during the various stages of its service life.

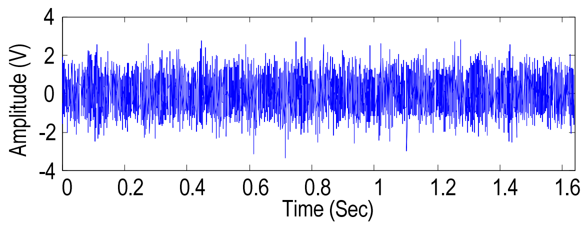

(a) Measured vibration signal

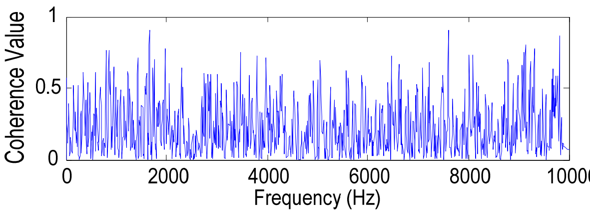

(b) Coherence function

Figure 1. Coherence function of a rotating spindle, showing no clear pattern of correlation between hammer strikes and the spindle's structural response.

Output-only modal analysis has been initiated and extensively studied in the area of civil engineering [8-14], due to the following advantages, such as: (1) Testing is relatively simple and fast, as no excitation equipment (e.g., vibration shaker or impact hammer) is needed; (2) Testing does not interfere with the operation of the structure, thus enabling in-situ testing; (3) Measured response is representative of the real operating conditions of the structure; and (4) this method is capable of identifying the same modal parameters as the traditional experimental modal analysis, except for not being able to estimate the stiffness of the structure. Of various techniques (e.g., the natural excitation technique [8,9], stochastic subspace identification [15], frequency domain decomposition [16], and random decrement technique [17]) used for output-only modal analysis, the stochastic subspace identification (SSI) technique has attracted increasing attention, and its application has been extended from civil engineering [18, 19] to aerospace [20, 21] and mechanical engineering [22, 23]. For example, the SSI technique was applied to in-flight data measured on a helicopter to validate and update its ground test models [20]. In another study, the SSI technique was used to analyze operational vibration data from a laser cutting machine. This study has revealed an additional mode of vibration with direct influence on the cutting results, which could not be identified by the classical modal analysis [22].

By utilizing advantages of the output-only modal analysis, and referring to successful application of the SSI approach, this paper presents an experimental investigation of SSI-based in-process modal parameter identification for rotating spindle condition monitoring under varying operation conditions. Instead of fitting an empirical model to the FRF from artificial excitations, only the spindle's measured output was used by the SSI technique to extract modal parameters [15, 20, 24]. This technique accounts for dynamic changes caused by the rotations of the spindle without the need for artificial excitations [11], and thus does not suffer from the inherently low signal-to-noise ratio typically associated with hammer-striking a rotating spindle as shown in Figure 1.

The rest of this paper is organized as follows. Section 2 introduces the theoretic formulation of the SSI-based technique, in which its ability to identify mode parameters of structures subject to general force input is verified analytically. The application of the technique to spindle condition monitoring is then conducted on a custom-designed spindle test system - an accelerated run-to-failure test discussed in detaile in Section 3. Finally, conclusions are drawn in Section 4.

2 Stochastic Subspace Identification

Stochastic subspace identification is a time-domain technique for output-only modal analysis, and is formulated using state-space models. Assuming that the vibrational behavior of a continual mechanical system (such as a spindle) can be analytically approximated by that of an equivalent, multiple degree-of-freedom (MDOF) system (e.g., a series of mass-spring-dampers), and the structural response is linear and time-invariant, the corresponding discrete state-space model of the spindle can be expressed as:

$$\begin{cases} x_{k+1} = Ax_k + Bu_k + w_k \\ y_k = Cx_k + Du_k + v_k \end{cases} \tag{1}$$

where $x_k=x(k\Delta t)$ is the discrete-time state vector, u_k is the structural input displacement vector resulting from a known excitation force, y_k is the system response vector, A is the state matrix, B is the input matrix, C is the output matrix, and D is the direct transmission matrix. The two components, w_k and v_k, represent the disturbance noise to the spindle and measurement noise due to sensor inaccuracy, respectively, and are stochastic in nature. The state space dimension n is determined by the number of independent variables needed to describe the physical system, i.e., the number of mass-spring-dampers as the constituent elements for spindle modeling. Given that no known excitation force is applied to the spindle when performing the natural input model analysis, the term u_k would vanish, and the system is then represented by the stochastic state-space model as [7,8]:

$$\begin{cases} x_{k+1} = Ax_k + w_k \\ y_k = Cx_k + v_k \end{cases} \tag{2}$$

Equation (2) indicates that the new state of the spindle physical system, x_{k+1}, can be obtained by the sum of the state matrix A (n×n) multiplied with the old state vector x_k (n×1) and the disturbance noise vector w_k (n×1). Thus the dynamics of the spindle are completely characterized by the state matrix A, and the modal parameters can be extracted from its eigenvalues. Also as shown in equation (2), the measured system response vector y_k (m×1) contains the observable part of the state vector Cx_k (m×1) and the measurement noise vector v_k (m×1), with m being the number of sensors used for the measurements.

In order to identify the state matrix A from the measured system response (vibrations of the spindle), an optimal estimator of the state-space model must be obtained based on the measured system response. This requires that such measured system response must be a Gaussian stochastic process with zero mean, which leads to

$$\begin{cases} E[y_k] = 0 \\ E[y_{k+i}y_k^T] = \Lambda_i \end{cases} \tag{3}$$

where Λ_i is the output covariance matrix describing the Gaussian stochastic process, i.e., the measured system response. This means once the state space model with the covariance matrix Λ_i can be estimated, it will completely describe the statistical properties of the measured system response. The corresponding estimator that can generate the state space model is then considered as the optimal estimator. Furthermore, equation (3) implies that the input noise processes w_k and v_k are also zero-mean Gaussian ($E[w_k]=0$ and $E[v_k]=0$), which are defined by the covariance matrices as:

$$E\left[\begin{pmatrix} w_p \\ v_p \end{pmatrix}\begin{pmatrix} w_q^T & v_q^T \end{pmatrix}\right] = \begin{pmatrix} Q & S \\ S^T & R \end{pmatrix}\delta_{pq} \tag{4}$$

where δ_{pq} is the Kronecker delta function, and Q, S, and R are the noise covariance matrices. Similarly, the state vector x_k is also zero-mean ($E[x_k]=0$) with the state covariance matrices and the updated state-output matrices defined using the noise covariance matrices as:

$$E[x_k x_k^T] = \Sigma = A\Sigma A^T + Q \tag{5}$$

$$E[x_{k+1} y_k^T] = G = A\Sigma A^T + S \tag{6}$$

Based on the covariance matrices defined in equations (4) to (6), the output covariance matrices can be rewritten as:

$$E[y_{k+i}\, y_k^T] = \begin{cases} \Lambda_0 = C\Sigma C^T + R & i = 0 \\ \Lambda_i = CA^{i-1}G & i \neq 0 \end{cases} \tag{7}$$

These covariance matrices are also called the system matrices because they describe the stochastic properties of the state-space systems. They are used for the estimation of the state-space model, and thus the identification of the state matrix *A*. Another system matrix needed for estimation is the extended observability matrix, which is defined as:

$$O_i \equiv \begin{pmatrix} C \\ CA \\ CA^2 \\ \cdots \\ CA^{i-1} \end{pmatrix} \tag{8}$$

Two types of algorithms are commonly employed for state-space model estimation: data-driven and covariance-driven algorithms [15]. For the presented study, a reference-based data-driven algorithm was investigated. A Kalman filter is employed for the optimal prediction of the state vector x_{k+1} by making use of the chosen reference sensor measurements, which is denoted as $\hat{x}_{k+1}$. A Kalman filter state sequence can be formed by the various Kalman filter state estimates as:

$$\hat{X}_i \equiv (\hat{x}_i\ \hat{x}_{i+1} \ldots \hat{x}_{i+j-1}) \tag{9}$$

Once the Kalman filter state estimates are obtained, numerical techniques can be applied to estimate the state-space model, e.g., using the QR-factorization technique [15], which essentially projects the row space of the future outputs into the row space of the past outputs. The projection can be factorized as the product of the observability matrix and the Kalman filter state sequences:

$$P_i = O_i \hat{X}_i \tag{10}$$

Thus, the Kalman filter state sequence is expressed as:

$$\begin{cases} \hat{X}_i = O_i^{-1} P_i \\ \hat{X}_{i+1} = O_{i-1}^{-1} P_{i-1} \end{cases} \tag{11}$$

By applying equation (11) and extending equation (2), the state-space spindle model is then obtained in the form of a set of linear equations:

$$\begin{pmatrix} \hat{X}_{i+1} \\ Y_{i|i} \end{pmatrix} = \begin{pmatrix} A \\ C \end{pmatrix} \hat{X}_i + \begin{pmatrix} \rho_w \\ \rho_v \end{pmatrix} \tag{12}$$

where $Y_{i|i}$ is the measured system responses written in the form of a block Hankel matrix and $(\rho_w\, \rho_v)^T$ are the residuals. Since the residuals are uncorrelated with $\hat{X}_i$, the system matrices *A* and *C* can be solved in equation (12) as:

$$\begin{pmatrix} A \\ C \end{pmatrix} = \begin{pmatrix} \hat{X}_{i+1} \\ Y_{i|i} \end{pmatrix} \hat{X}_i^{-1} \tag{13}$$

Since the dynamic behavior of the spindle is represented by the state matrix *A*, the eigen-frequencies and modal damping ratios can be obtained from the eigenvalues of state matrix *A*, using known decomposition techniques.

It should be noted that the SSI-based output-only modal analysis can also be extended to deal with applications where they don't satisfy the condition requirement of white noise input, which is often the case encountered in mechanical systems. This is achieved by assuming that the white noise input drives a virtual loading structure to generate force input to the structure of interest [25], e.g., the spindle, as illustrated in Figure 2. With this representation, the measured response contains information on dynamics of both the loading structure and the spindle, thus the corresponding identification process includes not only the vibration modes associated with the structure of interest itself, but also the modes that belong to the virtual loading structure. However, the modal parameters of the structure of interest are separable from those of the virtually excited modes of the loading structure. This is verified as follows.

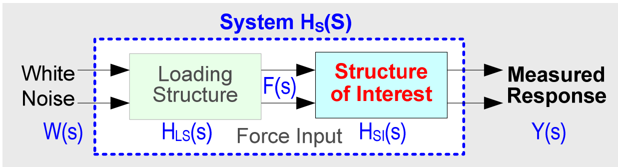

Figure 2. Illustration of output-only identification system.

Based on the illustration shown in Figure 2, the following relationship can be obtained as:

$$\begin{cases} F(s) = W(S) \cdot H_{LS}(S) \\ Y(S) = F(S) \cdot H_{SI}(S) \end{cases} \tag{14}$$

where *W*(*S*) denotes the white noise input, *F*(*S*) is the force generated from the loading structure and applied to the structure of interest. *Y*(*S*) is the measured system response. $H_{LS}(S)$ and $H_{SI}(S)$ are the transfer function of the loading structure and the structure of interest, respectively. The transfer function $H_S(S)$ of the system is defined as:

$$H_S(s) = Y(s)/W(s) \tag{15}$$

Combining equation (14) with equation (15), the system's transfer function can also be expressed as:

$$H_S(s) = H_{LS}(s) \cdot H_{SI}(s) \tag{16}$$

Suppose there are *n* and *m* modes for the loading structure and structure of interest, respectively, the transfer function $H_{LS}(S)$ and $H_{SI}(S)$ can be expressed as:

$$H_{LS}(S) = \sum_{i=1}^{2n} \frac{a_i}{s - \alpha_i} \tag{17}$$

$$H_{SI}(S) = \sum_{j=1}^{2m} \frac{b_j}{s - \beta_j} \tag{18}$$

Substituting equations (17) and (18) into equation (16), the transfer function of the system can be further expressed as:

$$H_s(S)=\sum_{i=1}^{2n}\frac{a_i}{s-\alpha_i}\sum_{j=1}^{2m}\frac{b_j}{s-\beta_j}=\sum_{i=1}^{2n}\sum_{j=1}^{2m}\frac{a_ib_j}{(s-\alpha_i)(s-\beta_j)}$$
$$=\sum_{i=1}^{2n}\sum_{j=1}^{2m}[\frac{a_ib_j}{(s-\alpha_i)(\alpha_i-\beta_j)}+\frac{a_ib_j}{(s-\beta_j)(\beta_j-\alpha_i)}] \quad (19)$$
$$=\sum_{i=1}^{2n}\frac{Aa_i}{s-\alpha_i}+\sum_{j=1}^{2m}\frac{Bb_j}{s-\beta_j}$$

where A and B are constant, and can be calculated as:

$$A=\sum_{j=1}^{2m}\frac{b_j}{\alpha_i-\beta_j} \quad (20)$$

$$B=\sum_{i=1}^{2n}\frac{a_i}{\beta_j-\alpha_i} \quad (21)$$

Equation (19) verifies that all of the modal parameters of the structure of interest can be identified using the SSI-based output-only modal analysis technique even though the requirement of white noise input is not satisfied. The only issue is to identify and eliminate those modes related to the virtual loading structure from the system, which can be done based on human knowledge.

3 Monitoring an Operating Spindle

A series of experiments was conducted on a spindle test system to evaluate the applicability of the SSI-based technique for monitoring an operating spindle. The spindle is supported by four 42 mm-angular contact ball bearings (Figure 3), which are mounted as a duplex pair with two bearings on each end of the spindle shaft. Two air cylinders applied constant and impulsive loads to the spindle, simulating static preload (e.g., when machining a workpiece under constant speed and feed) and shock load (e.g., when impacted due to tool-workpiece collision) to the spindle. Eight sensor positions, denoted 1-8 in Figure 3, were chosen for measurements. The odd numbers specify measurement in the horizontal direction, and the even numbers along the vertical direction.

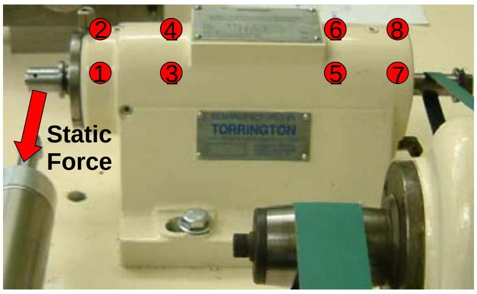

Figure 3. Spindle test-system setup and sensor positions.

The sampling frequency of the data acquisition board was set at 20,000 Hz, with the cut-off frequency of the anti-aliasing filter being 10,000 Hz. For stochastic subspace identification, the input noise terms are usually assumed to be white. It was observed from preliminary experiments that the rotating spindle also contains certain dominant frequency components, such as the spindle rotational frequency and bearing characteristic frequencies. These frequency components cannot be separated from the eigen-frequencies of the system, and thus will appear as poles of the state matrix A. On the other hand, it was noted that the highest dominant frequency of the spindle (ball passing frequency for inner raceway of the bearing) and its harmonics that contain noticeable energy content were all below 2,000 Hz, for the highest spindle speed investigated (879 rad/s or 8,400 rpm). To simplify data analysis, the measured vibration signals were first high-pass filtered at 2,000 Hz, in order to focus on spindle behavior within the frequency range of 2,000 Hz to 10,000 Hz, which is the Nyquist frequency.

3.1 Effect of dynamic impact

To investigate the effect of shock load to the spindle at the various stages of its service life, impact tests were conducted. Impacts of 13,300 N in magnitude and 25 ms in duration were consecutively applied to the spindle shaft, under a constant rotational speed of 377 rad/s (3,600 rpm), for a total of 1,100 times. Vibration signals were collected before the impact test and at 400 impacts, 700 impacts, and 1,100 impacts, respectively, without interrupting the operation of the spindle. To study the effects of speed and load, other rotational speeds (126 rad/s (1,200 rpm), 630 rad/s (6,000 rpm), and 879 rad/s (8,400 rpm)) and static loads (70 N, 419 N, 839 N, and 1,258 N) were also applied while measuring the signals.

Modal analysis of the spindle was subsequently performed using the SSI method described above. Since the true model order, i.e., the exact state space dimensions of the system, is unknown, a range of candidate state space models were used. To ensure accuracy, the number of dimensions was over-specified (i.e., 80) initially, and the appropriate dimension was iteratively determined to extract the modal parameters. The estimated models were plotted in the stabilization diagram. An example of such a diagram for the measured data under 126 rad/s (1,200 rpm) speed, no static load, and after 700 dynamic impacts is shown in Figure 4, where the estimated eigen-frequencies for each state space dimension is shown with the cross markers along the frequency axis.

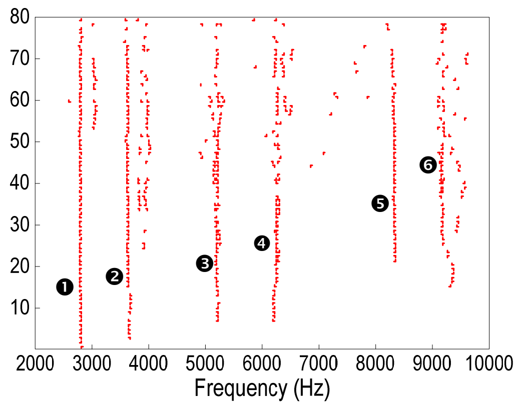

Figure 4. Stabilization diagram for the data set of 1200 rpm speed and no static load.

For the SSI analysis, noise (computational) modes are also estimated in addition to the structural modes. These noise modes are results of the non-fulfilled assumptions made by the algorithm itself. Typically, noise modes are spread in a non-repeated way and can be eliminated by establishing a threshold for damping ratio, typically 5%. This is because the structural modes are usually lightly damped (e.g., spindle damping ratio was found to be less than 4%); whereas the noise modes are more heavily damped. Furthermore, the structural modes would appear “stable” across the various state space dimensions with the estimated modal parameters. As shown in Figure 4, there are six stable modes presented in the diagram, between 2,000 Hz and 10,000 Hz. The modal parameters can then be obtained by either finding one state space dimension where all modes are stable or by choosing different dimensions to determine each individual mode.

Using the SSI method, the natural frequencies and the spectral densities of the spindle were estimated for all data sets collected during the impact tests. Figure 5 shows a comparison of the estimated spectral densities (solid lines) with the measured spectral densities (dotted lines) for the data sets for 126 rad/s (1,200 rpm) speed and no static load. Good agreement was found in the frequency range from 2,000 Hz to 10,000 Hz.

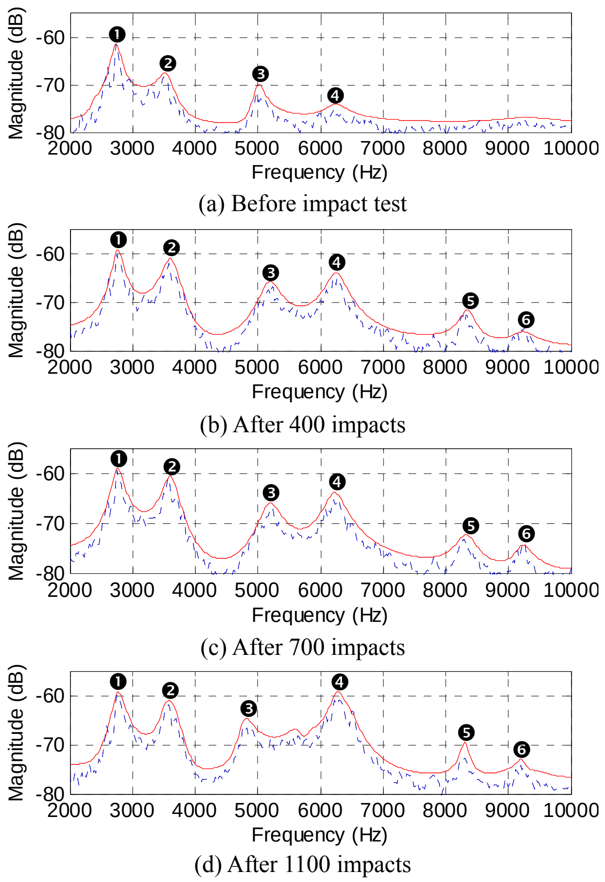

(a) Before impact test

(b) After 400 impacts

(c) After 700 impacts

(d) After 1100 impacts

Figure 5. Comparison of the estimated spectral density with the measured spectral density for the data set of 126 rad/s (1200 rpm) speed and no static load.

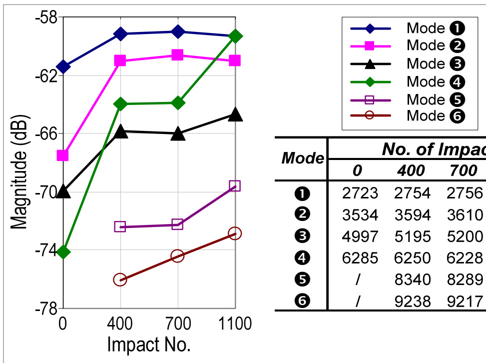

Mode	No. of Impacts			
	0	400	700	1100
❶	2723	2754	2756	2782
❷	3534	3594	3610	3588
❸	4997	5195	5200	4833
❹	6285	6250	6228	6268
❺	/	8340	8289	8308
❻	/	9238	9217	9244

Figure 6. Change of spindle natural frequencies as a function of the impacts, obtained at 126 rad/s (1200 rpm).

It is apparent that the dynamics of the spindle have changed as a result of the accumulated impacts. Before the impact application, when the spindle is defined as in a “healthy” state, the spectrum showed only four structural modes being identified, as shown in Figure 5(a). After 400 impacts, two additional modes appeared in the frequency range of 8,000 Hz to 10,000 Hz. The magnitudes of these two modes increased with an increasing number of the impacts. In addition, the magnitude of mode ❹ also has appeared to be increasing. The estimated natural frequencies and the change of their magnitudes with impact numbers at different stages of the impact tests are listed in Figure 6.

A wavelet enveloping analysis was then conducted to investigate the condition of the spindle after 700 impacts [26]. As shown in Figure 7, several characteristic frequencies associated with the spindle unbalance and bearing inner raceway defect were detected successfully, indicating such damages have been developed on the spindle as the impacts accumulated. It is thus concluded that the change of the spindle dynamics is the result of the structural damage. The data sets collected for other speed-load combinations also showed the same change of spindle dynamics. Further impact tests are being conducted, and it is expected that they will help reveal more conclusively the nature of the changes.

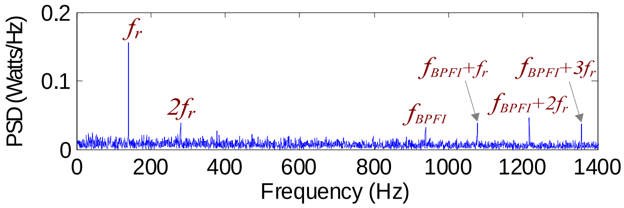

Figure 7. Wavelet envelope spectrum of the vibration signal measured after 700 impacts.

3.2 Effect of loading

To study the effect of static loading on the spindle dynamics, the natural frequencies for four loading conditions were extracted, under four different speeds. Data sets were collected after 700 impacts. It was found that for all six modes identified in Figure 5, the natural frequencies show an increasing trend, as the static load increases. Examples are given in Figure 8, illustrating changes of the natural frequencies for modes ❶ and ❺.

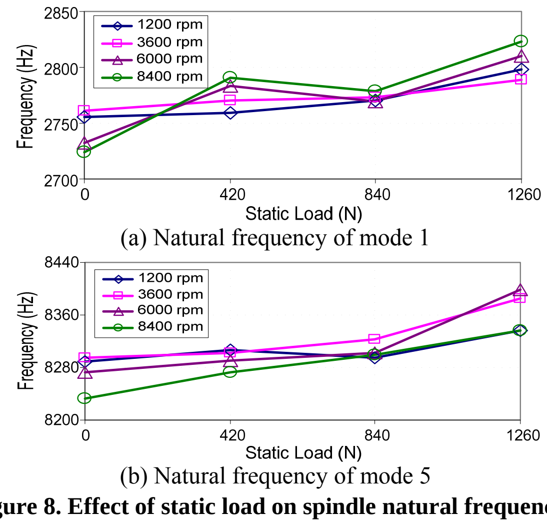

(a) Natural frequency of mode 1

(b) Natural frequency of mode 5

Figure 8. Effect of static load on spindle natural frequencies related to modes❶ and ❺.

A similar trend was identified for other structural modes. This can be explained in that increased static load has led to increased stiffness of the spindle structure and thus the natural frequencies. Such a finding is in agreement with the investigations reported in [5] and [6]. Further experiments are planned to improve the accuracy of the analysis.

4 Conclusions

The output-only modal analysis technique has been studied to identify changes of spindle dynamics due to load and speed variations, at various stages in its service life. Such a technique does not require known inputs to the spindle, and is performed when the spindle is under realistic operation conditions. It therefore accounts for structural excitations, which are not considered if the spindle remains stationary during experiments using hammer strikes. Using the stochastic subspace identification (SSI) algorithm, a series of vibration signals measured on a custom-designed spindle test system was analyzed. Modal parameter changes were identified as a result of the accumulated impacts on the spindle. The technique presents a new, complementary approach to analyzing a spindle's structural dynamics, and the information obtained provides insight into its present working status and future performance.

References

1. Shamine, D.M. et al, Experimental identification of dynamic parameters of rolling element bearings in machine tools, *ASME Journal of Dynamic Systems, Measurement, and Control*, 122(1):95-101, 2000.
2. Park, S. S. and Altintas, Y., Dynamic compensation of spindle integrated force sensors with Kalman filter, *ASME Journal of Dynamic Systems, Measurement, and Control*, 126(3):443-452, 2004.
3. Park, S. S. and Altintas, Y., Identification of spindle integrated force sensor's transfer function for modular end mills, In: *Proceedings of the ASME Manufacturing Engineering Division*, 14:113-120, 2003.
4. Yamamoto, T. and Ishida, Y., Particular vibration phenomena due to ball bearings at the major critical speeds, *Bulletin of the Japan Society of Mechanical Engineers*, 17(103):59-67, 1974.
5. Akturk, N., Some characteristic parameters affecting the natural fFrequency of a rotating shaft supported by defect free ball bearings, *Proceedings of the Institute of Mechanical Engineers, Part K: Journal of Multi-body Dynamics*, 217(2):145-151, 2003.
6. Alfares, M.A. and Elsharkawy, A.A., Effects of axial preloading of angular contact ball bearings on the dynamics of a grinding machine spindle system, *Journal of Materials Processing Technology*, 136:48-59, 2003.
7. Zhang, L., Yan, R., Gao, R., and Lee, K., Open architecture software design for online spindle health monitoring. In: *Proceedings of the 2007 IEEE Instrumentation & Measurement Technology Conference*, Warsaw, Poland, May 1-3, 2007.
8. James, G.H., et al, Modal testing using natural excitation, In: *Proceedings of the 10th IMAC*, CA, USA, 1992.
9. James, G.H., Carne, T.G., and Lauffer, J.P., The natural excitation technique (Next) for modal parameter extraction from operating structures, *International Journal of Analytical and Experimental Modal Analysis*, 10(4):260-277, 1995.
10. Kirkegaard, P.H. and Andersen, P., State space identification of civil engineering structures from output measurements, In: *Proceedings of SPIE*, 3089:889-895, 1997.
11. Tasker, F., Bosse, A., and Fisher, S., Real-time modal parameter estimation using subspace methods: theory, *Mechanical Systems and Signal Processing*, 12:795-806, 1998.
12. Ren, W. and Zong, Z., Output-only modal parameter identification of civil engineering structures, *Structural Engineering and Mechanics*, 19(3-4):1-16, 2004.
13. Kim B. H., Stubbs, N., and Park, T., A new method to extract modal parameters using output-only responses, *Journal of Sound and Vibration*, 282:215-230, 2005.
14. Fan, J., Zhang, Z., and Hua, H., Data processing in subspace identification and modal parameter identification of an arch bridge, *Mechanical Systems and Signal Processing*, 21(4):1674-1689, 2007.
15. Peeters, B. and De Roeck, G., Reference-based stochastic subspace identification for output-only modal analysis, *Mechanical Systems and Signal Processing*, 13(6):855-878, 1999.
16. Brincker, R., Zhang, L., and Andersen, P., Modal identification from ambient response using frequency domain decomposition, In: *Proceedings of the 18th IMAC*, TX, USA, 2000.
17. Ibraham, S.R., Efficient random decrement computation for identification of ambient responses, In: *Proceedings of the 19 IMAC*, FL, USA, 2001.
18. Hermans, L. and Van Der Auweraer, H., Model testing and analysis of structures under operational conditions: industrial applications, *Mechanical Systems and Signal Processing*, 13(2):193-216, 1999.
19. Mevel, L. and Goursat, M., Stochastic subspace-based structural identification and damage detection and localization – application to the Z24 bridge benchmark, *Mechanical Systems and Signal Processing*, 17(1):143-151, 2003.
20. Basseville M., et al, Output-only subspace-based structural identification: from theory to industrial testing practice, *ASME Journal of Dynamic Systems, Measurement, and Control*, 23:668-676, 2001.
21. Mevel, L. et al, Input/output versus output-only data processing for structural identification – application to in-flight data analysis, *Journal of Sound and Vibration*, 295:531-552, 2006.
22. Schedligski, C. and Lüscher, M., Application of classical and output-only modal analysis to a laser cutting machine, In: *Proceedings of ISMA*, 2002.
23. Kushnir, E., Application of operational modal analysis to a machine tool testing, In: *Proceeding of ASME International Mechanical Engineering Congress and Exposition*, CA, USA, 2004.
24. Peeters, B. and De Roeck, G., Stochastic system identification for operational modal analysis: a review, *ASME Journal of Dynamic Systems, Measurement, and Control*, 123:659-667, 2001.
25. Ibrahim, S.R., Brincker, R., Asmussen, J.C., Modal parameter identification from responses of general unknown random inputs, In: *Proceedings of he 14th IMAC*, MI, USA, pp. 446-452, 1996.
26. Zhang, L., Gao, R., and Lee, K., Spindle health diagnosis based on analytic wavelet enveloping, *IEEE Transactions on Instrumentation and Measurement*, 55(5):1850-1858, 2006.